The global characteristics of the three-dimensional thermal convection inside a spherical shell

J. Arkani-Hamed

Nonlinear Processes in Geophysics (1997) 4: 19–27

Nonlinear Processes in Geophysics

The global characteristics of the three-dimensional thermal convection inside a spherical shell

J. Arkani-Hamed

Earth and Planetary Sciences, McGill University, Montreal, Quebec, Canada

Received 30 July 1994 - Revised 15 April 1996 - Accepted 17 January 1997

Abstract. The Rayleigh number-Nusselt number, and the Rayleigh number-thermal boundary layer thickness relationships are determined for the three-dimensional convection in a spherical shell of constant physical parameters. Several models are considered with Rayleigh numbers ranging from 1.1×10^2 to 2.1×10^5 times the critical Rayleigh number. At lower Rayleigh numbers the Nusselt number of the three-dimensional convection is greater than that predicted from the boundary layer theory of a horizontal layer but agrees well with the results of an axisymmetric convection in a spherical shell. At high Rayleigh numbers of about 10^5 times the critical value, which are the characteristics of the mantle convection in terrestrial planets, the Nusselt number of the three-dimensional convection is in good agreement with that of the boundary layer theory. At even higher Rayleigh numbers, the Nusselt number of the three-dimensional convection becomes less than those obtained from the boundary layer theory. The thicknesses of the thermal boundary layers of the spherical shell are not identical, unlike those of the horizontal layer. The inner thermal boundary is thinner than the outer one, by about 30-40%. Also, the temperature drop across the inner boundary layer is greater than that across the outer boundary layer.

1 Introduction

The thermal boundary layer theory is developed in order to estimate heat transfer through an incompressible horizontal layer of constant physical parameters by steady state thermal convection (Turcotte and Oxburgh, 1967). For fixed temperatures at the upper and lower surfaces, the theory assumes that the interior of the layer is subdivided into three distinct regions: two thermal boundary layers, one at the top and the other at the bottom, where convective velocity is horizontal and thus the vertical heat transfer is solely by conduction, and the middle isothermal region where heat transfers by convection alone. Due to symmetry, the two boundary layers have identical thicknesses and temperature gradients. The efficiency of heat transfer denoted by the Nusselt number, Nu (which is the ratio of surface heat flux of a convecting layer to that of an identical but conducting layer), and the thickness of a thermal boundary layers, δ , are related to the Rayleigh number, $\mathbf{R_a}$, of the convection through the following power laws (Jarvis and Peltier, 1989):

$$\mathrm{Nu} = 0.93 \left(\frac{\mathbf{R_a}}{\mathbf{R_c}}\right)^{1/3} \tag{1}$$

and

$$\delta = 0.465 \left(\frac{\mathbf{R_a}}{\mathbf{R_c}}\right)^{-1/3} \tag{2}$$

where

$$\mathbf{R_a} = \frac{\mathrm{C_p g \alpha \rho^2 \Delta T D^3}}{\mathrm{K}\eta} \tag{3}$$

and $\mathbf{R_c}$ is the critical Rayleigh number. In Eq.(3) $\mathrm{C_p}$ is the specific heat, g is the gravitational acceleration, α is the thermal expansion coefficient, ρ is the density, ΔT is the total temperature drop across the layer, D is the thickness of the layer, K is the thermal conductivity, and η is the dynamic viscosity. However, in a convecting layer the velocity vector does have a vertical component within a thermal boundary layer, and the boundary between the isothermal interior and a thermal boundary layer is not sharp. This is specially so for a low-Rayleigh number convection. Moreover, a thermal boundary layer with dominantly horizontal velocity thickens as a distance from the stagnation regions of the convection circulations. The constant thickness expressed by Eq.(2) is an effective thickness

Correspondence to: J. Arkani-Hamed

regarding a single convection cell. The numerical solution of the dynamic equations of steady state thermal convection in a horizontal layer of constant physical parameters also results in power-law relationships between the Nusselt number and the Rayleigh number, and between the mean thermal boundary layer thickness and the Rayleigh number, but with slightly different values of the constants and exponents in the above equations, possibly due to different aspect ratios of convection cells (e.g., Jarvis and Peltier, 1989). This emphasizes that the boundary layer theory provides a good approximation for the major characteristics of thermal convection in a horizontal layer of constant physical parameters.

Modified versions of the boundary layer theory where the thickness of the thermal boundary layer is determined by the local Rayleigh number has been used to calculate the heat transfer through the mantles of terrestrial planets in order to determine the overall cooling of their cores (Stevenson et al., 1983). Davies(1993) applied the boundary layer theory to study the cooling of the Earth's core. The boundary layer theory was also used to examine the possibility of mantle overturn in Venus where the upper mantle and the lower mantle were assumed to replace each other from time to time (Herrick and Parmentier, 1994). Aside from the fact that the physical parameters of the mantles are certainly not constant, the mantles of the planets are thick and the radii of curvature of the surface and the core-mantle boundary are quite different, by a factor of about 2 in the case of the Earth. Detailed studies of convection inside cylindrical and spherical shells with different radii of curvature of the upper and lower surfaces show that the lower thermal boundary layer is thinner than that of the upper one (Jarvis, 1994; Vangelov and Jarvis, 1994). This implies that the core of the planets may cool much faster than that predicted by the boundary layer theory derived for a horizontal layer.

The relationships between the Rayleigh number and the thermal boundary layer thickness, and between the Rayleigh number and the Nusselt number, have been investigated in some detail for thermal convection inside a spherical shell of constant physical parameters using axisymmetric convection calculations (Vangelov and Jarvis, 1994). The calculations were limited to Rayleigh numbers up to about 14,000 times the critical value which is about an order of magnitude smaller than the Rayleigh number of the Earth's mantle at present. Solheim and Peltier's (1990) axisymmetric model with constant density and no internal heating considered Rayleigh numbers as high as 4×10^4 times the critical value. However, the convection in the planetary mantles is most likely three-dimensional with high Rayleigh numbers. The present paper investigates the relationships between the Rayleigh number and the thermal boundary layer thickness, and between the Rayleigh number and the Nusselt number, which are derived from solving the three-dimensional thermal convection equations inside a spherical shell. Moreover, the Rayleigh numbers considered are as high as 2.1×10^5 times that of the critical value, and thus are suitable for thermal convection inside the planetary mantles. The shell is assumed to have constant physical parameters in order to single out the effects of the different curvatures of the core-mantle boundary and the surface on the heat transfer through the shell, and to compare our results with those of the horizontal layer and the axisymmetric spherical shell models. For the same reason, no radioactive or viscous heating is considered and the temperature at the core-mantle boundary is fixed. It is shown in this paper that the boundary layer theory derived for a horizontal layer somewhat overestimates the cooling of the planetary mantle, but substantially underestimates the cooling of the planetary core.

2 Three-dimensional convection in a spherical shell

This section investigates the relationship between the Rayleigh number and the Nusselt number and between the Rayleigh number and the thermal boundary layer thickness of the three-dimensional thermal convection inside an incompressible spherical shell of constant physical parameters with fixed temperatures at the inner and outer surfaces and with no internal heating. The basic equations are the conservation of mass,

$$\nabla \cdot \mathbf{V} = 0, \tag{4}$$

the equation of motion, assuming an infinite Prandtl number and Newtonian viscosity,

$$\eta \nabla^2 \mathbf{V} - \nabla \pi + \mathbf{R_a} g \alpha \mathrm{T} \mathbf{r} = 0, \tag{5}$$

and the energy equation

$$\left(\frac{\partial}{\partial \mathrm{t}} + \mathbf{V} \cdot \nabla \right) \mathrm{T} - \mathrm{k} \nabla^2 \mathrm{T} = 0, \tag{6}$$

where $\mathbf{V}$ is the velocity vector, π is the perturbations of pressure, T is temperature, t is time, k is the thermal diffusivity, and $\mathbf{r}$ is the unit vector along the radius r. $\mathbf{R_a}$ is the Rayleigh number as defined by Eq.(3) where D now is the thickness of the shell and ΔT is the difference between the temperature at the inner surface, $\mathrm{T_1}$, and that at the outer surface, $\mathrm{T_2}$, of the shell, i.e., $\Delta \mathrm{T} = \mathrm{T_1} - \mathrm{T_2}$. The equations are solved by a bi-harmonic method, using stress-free and isothermal boundary conditions at the inner and outer surfaces of the shell. The lateral dependencies of temperature and velocity fields are expressed in terms of spherical harmonics including harmonics of degree and order up to 9 inclusive (a total of 100 harmonics). The radial dependencies are determined through the numerical solution of the resulting second order integrodifferential equation of motion and the energy equation, using a finite difference technique (Arkani-Hamed and Toksoz,

1984). There are 44 unequally spaced grid points in the radial direction, with shorter spacing inside the upper and lower thermal boundary layers. From the surface toward the interior in both the upper and lower 100 km, there are 4 layers of thicknesses 20, 20, 30, and 30 km, respectively. The effects of the grid resolution will be discussed later.

The spherical shell considered in this study is a reasonable model for the Earth's mantle as far as its dimension and average physical parameters are concerned. It has an outer radius of $R_2 = 6370$ km, an inner radius of $R_1 = 3470$ km, a density of 4460 Kg/m^3, a thermal expansion coefficient of 3×10^{-5}K^{-1}, a thermal conductivity of K=5.748 W m^{-1}K^{-1} (this is an estimate of the mean thermal conductivity of the Earth's mantle, assuming olivine rich material and taking into account its temperature dependence (Schatz and Simmons, 1972)), and a specific heat of 1200 J kg^{-1}K^{-1}. The gravitational acceleration is determined assuming a core with a uniform density of 1100 kg/m^3. The outer surface temperature is put to zero and that at the inner surface is assumed to be 2500°C. We calculate several models with identical physical parameters except for their viscosities. Table 1 lists the models, their viscosities and Rayleigh numbers. The Rayleigh numbers span a range of 1.1×10^2 to 2.1×10^5 times the critical value of 711 (Solheim and Peltier, 1990). The higher values are appropriate for the convection in the planetary mantles.

Each model starts with a high temperature distribution and calculations are continued until the model reaches a statistically steady state (many of the models show oscillatory behaviour, but resemble steady states in their overall properties, i.e. they are statistically steady state), which will be briefly called steady state hereafter. A given model is initially perturbed by a small amplitude velocity field. We monitor the surface heat flux, the heat flux at the inner surface, and the kinetic energy spectra of the convection, all of which either become time independent or oscillate about constant mean values, implying that the model has reached a statistically steady state condition. Figure 1 shows the laterally averaged temperature distribution inside model M_2 at certain times. The model has a low viscosity of 10^{21} Pa s, which is similar to the viscosity of the Earth's upper mantle but lower than that of the lower mantle. In a relatively short time period, a strong thermal boundary layer develops near the inner surface while the interior part becomes isothermal. The main features of the temperature distribution are similar to those of the horizontally averaged temperature distribution inside a convecting horizontal layer. However, in the spherical shell, with an inner surface area that is about 25% of the outer surface area, a substantially enhanced boundary layer is developed at the base compared to that at the surface. Not only the total temperature drop across the lower thermal boundary layer is greater than that across the upper boundary layer,

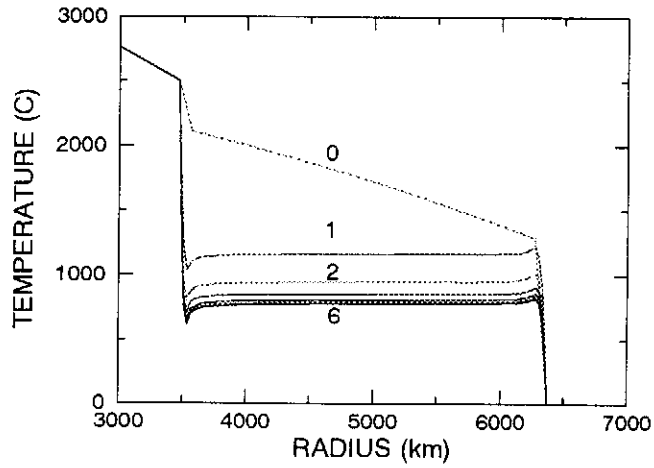

Fig. 1. Laterally averaged temperature distribution in model M_2. The numbers on the curves show the time in b.y.

but also the lower boundary layer is thinner than the upper one, so that the total heat flow through the inner surface is equal to that through the outer surface.

Figure 2a shows the heat flux at the upper surface of the models versus time, demonstrating that all models reach steady state conditions. Models M_1, M_2, M_3, and M_4 oscillate about mean values (the low frequency oscillation of model M_1 compared to those of the other models is an artifact. In the computer programming, we output the results of computation at every 0.2 b.y. in this model, rather than at 0.02 b.y. used for the other models). As mentioned earlier, all of the models are initially perturbed by a small velocity field. The initial velocity of the high viscosity models M_7 and M_8 diminishes in time, allowing the temperature in the interior to reach an almost steady state conduction profile and resulting in the monotonic decay of the heat flux at the upper surface in the first about 3.5 b.y. Then, the instability suddenly develops and convection starts which substantially increases the heat flux in the early stages. The heat flux, however, decays to a constant value as time passes. The same models were also recalculated using initial perturbations in the temperature field. The developments in the early stages were different from those shown in Fig.2a, but as time passed they converged to steady state conditions similar to those seen in the figure. Figure 2b shows the time variations of the ratio of the total heat flow at the bottom to that at the top for some of the models, indicating that the ratios approach unity as time passes. Figures 2a and 2b suggest that the models reach steady state conditions during the time considered.

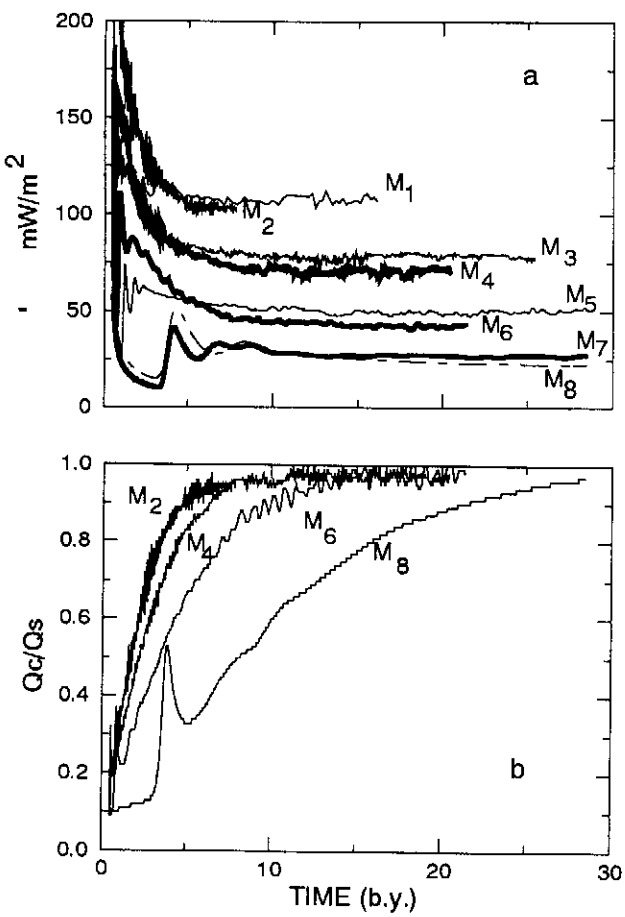

Fig. 2. a) Time variations of the surface heat flux of the three-dimensional models. b) Time variations of the heat flow at the inner surface of the shell normalized to that at the outer surface for the three-dimensional models.

2.1 Thermal boundary layers

There is no consensus among investigators about the definition of the thickness of a thermal boundary layer. McKenzie (1977) considered the intersection of the interior isotherm with a constant gradient temperature profile which is tangent to the laterally averaged temperature at the surface. Hansen and Ebel (1984) defined the boundary layer thickness as the distance from the surface to where the temperature reaches the interior isotherm. Jarvis and Peltier (1989) used two different definitions, the intersection of the extrapolated interior isotherm with the actual temperature profile in a boundary layer, and the depth to a local maximum (or minimum) of the laterally averaged temperature distribution. Jarvis (1994) assumed the interior surface of the boundary layer at the place where the advective heat flux equals the conductive heat flux. McKenzie's definition yields the thinnest boundary layer, while the local maximum (or minimum) criterion results in the thickest boundary layer. To account for the slightly nonlinear profiles of the laterally averaged temperature in the thermal boundary layers, I determined the thickness of the boundary layer from the intersection of the interior isotherm with a quadratic profile fitted to the laterally averaged temperature values of the outer parts of the thermal boundary layer. The resulting boundary layer thickness falls within between Jarvis and Peltier's (1989) first definition and Jarvis' (1994) definition. The differences of the thicknesses obtained using these three definitions are minor. Therefore, in this paper two boundary layer thicknesses are calculated, one using McKenzie's definition and the other using the thicker boundary layer definition of Jarvis and Peltier (1989), in order to include the two end members.

Figure 3a shows the relationship between the thickness of the boundary layer d (normalized to the thickness of the shell D) and the Rayleigh number $\mathbf{R_a}$ (normalized to the critical value $\mathbf{R_c} = 711$) for our models. The thickness decreases with the increase of the Rayleigh number, obeying a slightly nonlinear relationship in the log log plot. Moreover, the lower boundary layer is thinner than the upper one, by about 30-40%, for all the models. This is in distinct contradiction with that obtained from the boundary layer theory derived for a horizontal layer where the two boundary layers have identical thicknesses. The boundary layer theory of a horizontal layer predicts the isothermal temperature of the interior to be the average of the bottom and top temperatures, whereas the three-dimensional models suggest a significantly lower value as also concluded by Vangelov and Jarvis (1994) for a two-dimensional axisymmetric spherical shell model. Included in the figure is the power law relationship between the thermal boundary layer thickness of the horizontal layer and the Rayleigh number calculated from Eq.(2). The slopes of the curves are, in general, similar to that of the power

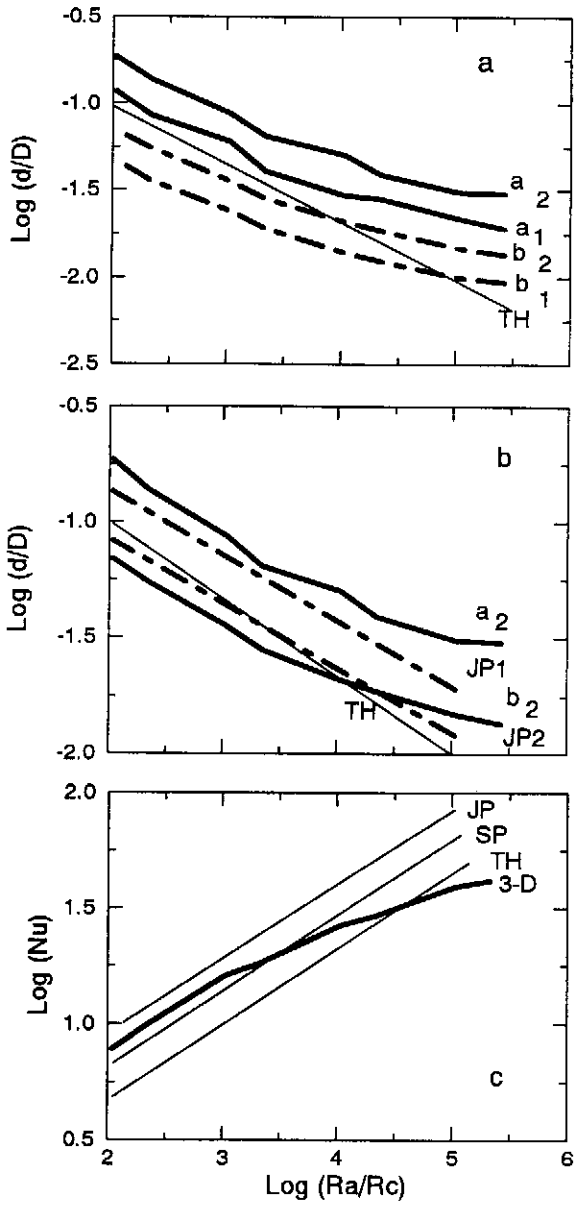

Fig. 3. a) The relationship between the thickness of the thermal boundary layers and the Rayleigh number $\mathbf{R_a}$. The curves denoted by a are determined using McKenzie's (1977) definition. Those denoted by b are computed using the thicker layer definition by Jarvis and Peltier (1989). The index 1 denotes the lower thermal boundary and index 2 the upper one. d is the thickness of the boundary layer and D is that of the spherical shell. $\mathbf{R_c}$ is the critical Rayleigh number. b) The relationship between the thickness of the upper thermal boundary layer and the Rayleigh number $\mathbf{R_a}$. The curve denoted by a is determined using McKenzie's (1977) definition. That denoted by b is computed using the thicker layer definition by Jarvis and Peltier (1989). d is the thickness of the boundary layer, D is that of the spherical shell, and $\mathbf{R_c}$ is the critical Rayleigh number. JP1 and JP2 are the boundary layer thicknesses determined by Jarvis and Peltier (1989), and TH is that of the horizontal layer computed by the boundary layer theory. c) The relationship between the Nusselt number and the Rayleigh number $\mathbf{R_a}$ for the three- dimensional models. $\mathbf{R_c}$ is the critical Rayleigh number. JP, SP, and TH are the power law relationships given by Jarvis and Peltier (1989), Solheim and Peltier (1990), and the boundary layer theory of a horizontal layer, respectively. JP and SP are linearly (in the log log plot) extrapolated to higher Rayleigh numbers. The dots are the fine-grid resolution models.

law for the low Rayleigh numbers. However, at higher Rayleigh numbers the curves become shallower.

Figure 3b shows the thickness of the upper thermal boundary layer of the three-dimensional models and those of the horizontal layer obtained from the power law of the boundary layer theory and the two power laws suggested by Jarvis and Peltier (1989) which are linearly extended to higher Rayleigh numbers for comparison. There is good agreement between our results and those of Jarvis and Peltier, especially for the slopes of the curves in the low Rayleigh number region. Our results, however, show a slightly non-linear relationship at higher Rayleigh numbers that is probably partly due to the coarser grid resolution in the boundary layers (see below).

2.2 The Nusselt number-Rayleigh number relationship

The Nusselt number of a model is proportional to its surface heat flux with a proportionality constant of $\gamma = [R_2(R_2 - R_1)]/(KR_1T_1)$, which is the inverse of the surface heat flux of the corresponding steady state conduction model (for the above parameter values $\gamma = 370.47$). Therefore, the time evolution of the Nusselt numbers of the models is similar to that of the surface heat flux (Fig.(2a)). In the following we discuss the Nusselt number-Rayleigh number relationship in a steady state, or statistically steady, convection.

The Nusselt number-Rayleigh number relationship of an axisymmetric convection inside a spherical shell significantly deviates from a power law (is strongly non-linear in the log log plot) at very low Rayleigh numbers (Machetel and Robinowicz, 1985). The Nusselt number increases monotonically as Rayleigh number increases, but suffers a sudden decrease at Rayleigh numbers of about 7-8 times the critical Rayleigh number. The configuration of the stream lines shows a transition from a 3 or 4 cell convection to a 2 cell convection at this Rayleigh number (Machetel and Robinowicz, 1985). According to axisymmetric models of Solheim and Peltier (1990), the Nusselt number-Rayleigh number relationship also shows significant changes at a higher Rayleigh number, between 500-1000 times the critical value, as convection changes from a steady state to a time-dependent oscillatory mode. At still higher Rayleigh numbers, up to about 4×10^4 times the critical value which is the highest value considered by Solheim and Peltier, the system is locked on to a power law relationship (linear in the log log plot). The models considered in this paper have much higher Rayleigh numbers than those studied by Machetel and Robinowicz, but includes the range of Rayleigh numbers modeled by Solheim and Peltier. The Nusselt number-Rayleigh number relationship of our models at the steady state condition deviates from a simple power law at high Rayleigh numbers, as it is shown on the log log plot in Fig.(3c) (see Table.1 for the Nusselt numbers at steady state conditions). Included

in the figure are the relationships obtained by Solheim and Peltier (1990) for an axisymmetric constant density spherical shell, by Jarvis and Peltier (1989) for a horizontal layer, and the one based on the boundary layer theory calculated from Eq.(1), all of which are linearly extended to higher Rayleigh numbers. Our models predict consistently lower Nusselt numbers than Jarvis and Peltier's model, and consistently higher than the model based on the boundary layer theory. But there is good agreement between Solheim and Peltier's and our results for the Rayleigh numbers up to about 10^4 of the critical value. This close agreement is due to the similar geometry of the models, both are spherical shells. At higher Rayleigh numbers, however, the heat transfer through the shell by a three-dimensional convection is less efficient than that predicted by linear extrapolation of the axisymmetric convection results of Solheim and Peltier (1990).

Determination of the Nusselt number strongly depends on the vertical resolution of the thermal boundary layers. At least 3 grid points are required to resolve a boundary layer of two-dimensional Rayleigh-Benard convection. The dependence on the grid resolution of the Nusselt number of a two-dimensional convection, with Rayleigh numbers up to 10^4 times the critical Rayleigh number, was examined in detail by Hansen and Ebel (1984) using vertically refined finite elements in the boundary layers compared to those in the isothermal interior. According to these authors, the Nusselt number does not change significantly as long as the vertical dimension of the boundary elements normalized to the total thickness of the layer, ε, remains smaller than 0.01, but strongly deviates for coarser grids, $\varepsilon = 0.02$ and 0.04. Hansen and Ebel's models correspond to our low-Rayleigh number models (M_5 to M_9). The layer thicknesses used in the upper and lower 100 km of our spherical shell models (20, 20, 30, and 30 km) correspond to the ε value of about 0.007, which is well within the range of 0.01-0.001 found to be acceptable by Hansen and Ebel for a low-Rayleigh number convection. However, the layer thicknesses are somewhat coarse for our high-Rayleigh number models M_1 to M_4, as seen from Table.1 which shows the boundary layer thickness estimated from the boundary layer theory, Eq.(2). To examine the effects of the vertical grid resolution of a boundary layer on the Nusselt number, the grid intervals are divided by 2, resulting in 88 grid points throughout the mantle. The layer thicknesses in the upper and lower 100 km are now 10, 10, 10, 10, 15, 15, 15, and 15 km from the surface toward the interior, respectively, which correspond to the ε value of about 0.0034. This ε value is well within the lower part of the range of 0.01-0.001, and according to Hansen and Ebel's conclusions the grid resolution of the models is now sufficient to produce reliable Nusselt numbers with negligible errors. Figure 4 shows the time evolution of the Nusselt number for the fine- and coarse-grid models. Aside from the early stages of strongly time-dependent circulations, the Nusselt numbers of the two identical models, but with different grid resolutions, converge to statistically steady states with a constant difference. The Nusselt numbers of the fine-grid models are greater than those of the coarser ones, the differences increase at higher Rayleigh numbers. We also ran our highest Rayleigh number model M_1 using the fine-grid resolution. However, the laterally averaged temperature of the final time step of the coarse-grid resolution model M_1 is used as an initial laterally averaged temperature distribution in this run, to save computer time. Figure 5 shows the time variations in the Nusselt number and the ratio of the total heat flow from the bottom to that across the surface for this run. Both curves show a very oscillatory behaviour, that is the main characteristic of convection at high Rayleigh numbers. Aside from oscillations, the figure shows that the run has achieved a statistically steady state.

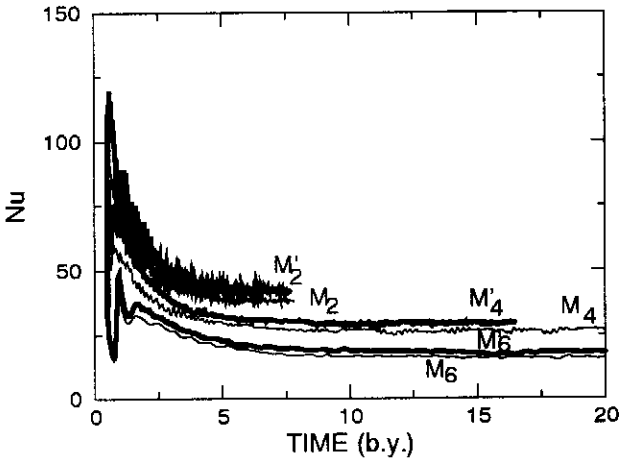

Fig. 4. Time variations of the Nusselt numbers of models M_2, M_4 and M_6. Primes denote the finer grid resolution models.

Included in Fig.(3c) are the average Nusselt numbers of the fine-grid models exhibiting a general trend as a function of the normalized Rayleigh number that is similar to the trend of the coarse-grid models. The Nusselt numbers of our models deviate from those of Solheim and Peltier at very high Rayleigh numbers and tend toward those predicted by the boundary layer theory. However, at higher Rayleigh numbers (2×10^5 times the critical value), that are characteristics of the mantle convection of the terrestrial planets in the early stages of their evolution, the Nusselt numbers are lower than the one predicted by the boundary layer theory. These relatively lower Nusselt numbers suggest that adopting a simple power-law relationship between the Nusselt number and the Rayleigh number derived from the boundary layer theory may overestimate the rate of cooling of the planets, especially during their early stages of evolution.

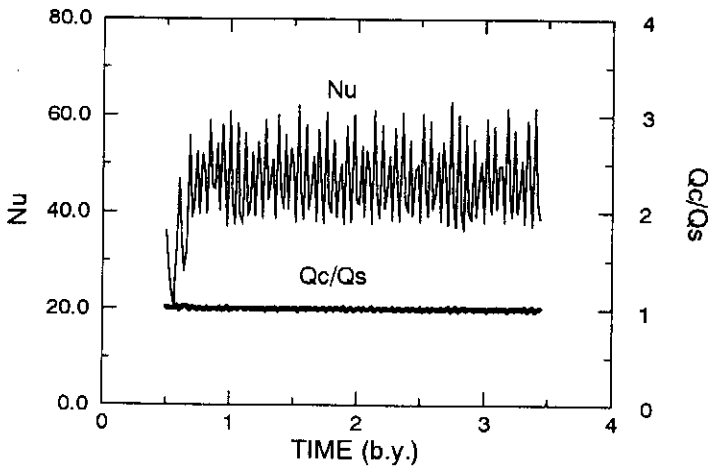

Fig. 5. Time variations of the Nusselt number and the ratio of the heat flux at the bottom to that at the top for the fine-grid resolution model M_1.

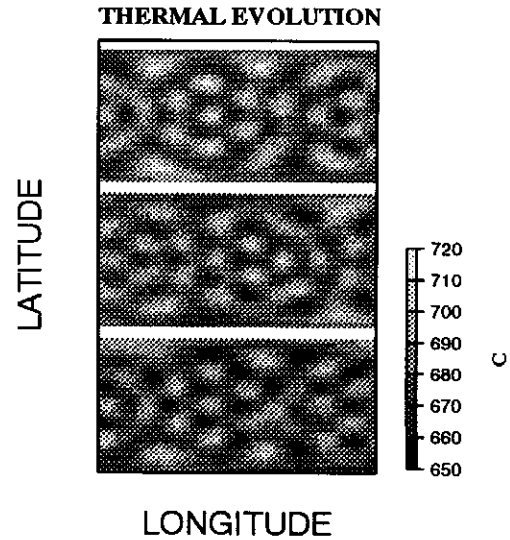

Fig. 6. Lateral temperature distribution on a spherical surface of radius 4000 km in the last 2 b.y. of model M_2. The lower panel is at the final time, the middle panel is at 1 b.y. earlier, and the top panel is at 2 b.y. earlier.

Another parameter that has a strong effect on the Nusselt numbers of the two-dimensional rectangular box convection models is the aspect ratio (the width to depth ratio) of the convection cells. According to the boundary layer theory, the Nusselt number is maximum for an aspect ratio of 1 (Turcotte and Schubert, 1982), whereas the numerical solutions of the dynamic equations result in a maximum Nusselt number at an aspect ratio of 0.7 (Olson and Corcos, 1980) or 0.8 (Hansen and Ebel, 1984). For aspect ratios higher than 1, models of different authors agree that the Nusselt number decreases with the increase of the aspect ratio. However, the whole aspect ratio idea is applicable to low-Rayleigh number, steady-state, and two-dimensional convection inside a rectangular box which is confined laterally. For convection inside a spherical shell, with no lateral confinement, the width of a cell changes (by a factor of about 2 in the Earth's mantle) due to the different curvatures of the lower and upper boundaries. Also, convection is strongly time-dependent at high Rayleigh numbers, both in a rectangular box (e.g., Jarvis and Peltier, 1989) and in an axisymmetric spherical shell (e.g., Solheim and Peltier, 1990). Hot (Cold) Plumes are generated almost randomly near the lower (upper) boundary with irregular aspect ratios and some lose their integrity as they ascend (descend) before reaching the top (bottom) boundary, the notion of aspect ratio loses its ground.

The aspect ratio idea has a qualitative importance when dealing with three-dimensional convection regardless of being in a rectangular box (Tackley, 1993) or in a spherical shell (Schubert et al, 1990). This is especially the case for high-Rayleigh number convection models which are strongly time-dependent. An aspect ratio only addresses the overall statistical characteristics of convection in time and space. This is demonstrated in Fig.(6) which shows the lateral temperature distribution on a spherical surface of radius 4000 km (i.e., at a depth of 2370 km which is almost the middle of the spherical shell) in the last 2 b.y. for the high-Rayleigh number model M_2 with a fine-grid resolution. Although the convection is time-dependent, its overall statistical feature which is characterised by cells of about 3000 km width (an approximate aspect ratio of about 1) changes only slightly. The figure also demonstrates the stability of the convection pattern even for the high-Rayleigh number model, indicating the stability of the numerical techniques adopted in this paper. This is partly due to the integrodifferential form of the numerical solution (Arkani-Hamed and Toksoz, 1984), the integral part tends to stabilize the solution.

The circulation pattern of convection strongly depends on the lateral resolution, i.e. the highest degree of spherical harmonics used in modelling the mantle circulations and lateral variations in the temperature distribution. Despite its great advantages of reducing the three-dimensional partial differential equation of motion of the thermal convection problem to a one-dimensional second order integrodifferential equation, the bi-harmonic technique utilized in this paper imposes strong computational limitations, both on memory and on CPU time. Consequently, our models suffer from their low lateral resolution, the highest degree harmonic used, n=9, has a wavelength of 3435 km at the middle of the mantle, the radius of 4920 km. However, the overall heat transfer through the mantle, and thus the Nusselt number, is mainly controlled by the long wavelength components

of mantle circulations (Jarvis and Peltier, 1986; Leitch and Yuen, 1991), suggesting that our models are probably adequate as far as the Nusselt number calculations are concerned.

3 Discussion and conclusions

The Earth's mantle is far from homogeneous. Not only are there chemical variations in lateral and radial directions, the physical parameters controlling the thermal evolution of the Earth, namely the rheology, density, thermal expansion coefficient, and thermal conductivity are temperature- and pressure-dependent and thus may significantly vary inside the mantle. The Newtonian rheology usually used in the thermal convection calculations for mathematical simplicity may not faithfully represent the mantle rheology. Moreover, the viscosity is strongly temperature- and pressure-dependent and may change by orders of magnitude laterally, by about an order of magnitude radially, and by more than an order of magnitude throughout the history of the Earth. It is plausible to assume that the mantle of other terrestrial planets are also heterogeneous. The application of convection models calculated using a homogeneous mantle with fixed temperatures at the lower and upper surfaces may not be viable. The core of a planet cools because of its limited energy budget, and the temperature at the core-mantle boundary decreases during the thermal evolution, substantially reducing the vigor of mantle convection and thus the cooling rate of the planet (Arkani-Hamed, 1994). In addition to these major shortcomings, the boundary layer theory developed based on convection in a horizontal layer, or the axisymmetric spherical shell convection models, overestimate the cooling rate of the planetary mantle. The three-dimensional thermal convection calculations presented in this paper show that the Nusselt numbers obtained at high Rayleigh numbers are lower than those predicted by the boundary layer theory or by an extrapolation of the results from axisymmetric models. It is also shown that, unlike the boundary layer theory of the horizontal layer, the inner thermal boundary layer of convection in a spherical shell is appreciably thinner than the outer one, by about 30-40%. Moreover, the temperature drop across the lower boundary layer is about 3 times that across the upper boundary layer. This suggests that the boundary layer theory substantially underestimates the cooling of the planetary core. Therefore, application of the boundary layer theory to mantle convection provides only a rough estimate of the thermal history of terrestrial mantles, but does not yield a reasonable assessment of the core cooling.

Acknowledgements. This research was supported by the Natural Sciences and Engineering Research Council (NSERC) of Canada, Operating Grant 0GP0041245. I would like to thank Gary Jarvis at York University for many constructive discussions.

References

Arkani-Hamed, J., Effects of the core cooling on the internal dynamics and thermal evolution of terrestrial planets, *J. Geophys. Res., 99*, 12,109-12,119, 1994.

Arkani-Hamed, J., and Toksoz M.N., Thermal evolution of Venus, *Phys. Earth and Planet. Inter., 34*, 232-250, 1984.

Hansen, U., and Ebel, A., Experiments with a numerical model related to mantle convection: boundary layer behaviour of small- and large scale flows, *Phys. Earth Planet. Int., 36*, 374-390, 1984.

Herrick, D.L., and Parmentier, E.M., Episodic large-scale overturn of two-layer mantle in terrestrial planets, *J. Geophys. Res., 99*, 2053-2062, 1994.

Jarvis, G.T., The unifying role of aspect ratio in cylindrical models of mantle convection with varying degrees of curvature, *Geophys. J. Int., 117*, 419-426, 1994.

Jarvis, G.T., and Peltier, W.R., Lateral heterogeneity in the convecting mantle, *J. Geophys. Res., 91*, 435-451, 1986.

Jarvis, G.T., and Peltier, W.R., Convection models and geophysical observations, in Mantle Convection: Plate Tectonics and Global Dynamics, W.R. Peltier, Ed., Gordon and Breach Science Publishers, 479-595, 1989.

Leitch, W.S., and Yuen, D.A., Compressible convection in a viscous Venusian mantle, *J. Geophys. Res., 96*, 15,551-15,562, 1991.

Machetel, P., and Robinowicz, M., Transitions to a two mode axisymmetrical spherical convection: Application to the Earth's mantle, *Geophys. Res. Lett., 12*, 227-230, 1985.

McKenzie, D.P., Surface deformation, gravity anomalies and convection, *Geophys. J. R. Astron. Soc., 48*, 211-238, 1977.

Oslon, P., and Corcos, G.M., A boundary layer model for mantle convection with surface plates, *Geophys. J. R. Astr. Soc., 62*, 195-219, 1980.

Schatz, J.F., and Simmons, G., Thermal conductivity of Earthmaterial at high temperatures, *J. Geophys. Res., 77*, 6966-6983, 1972.

Schubert, G., Bercovici, D., and Glatzmaier, G.A., Mantle Dynamics in Mars and Venus: Influence of an immobile lithosphere on three-dimensional mantle convection, *J. Geophys. Res., 95*, 14,105-14,129, 1990.

Solheim, L.P., and Peltier, W.R., Heat transfer and the onset of chaos in a spherical axisymmetric, inelastic model of whole mantle convection, *Geophys. Astrophys. Fluid Dynamics, 53*, 205-255, 1990.

Stevenson, D.J., Spohn, T., and Schubert, G., Magnetism and thermal evolution of the terrestrial planets, *Icarus, 54*, 466-489, 1983.

Tackley, P., Effects of strongly temperature-dependent viscosity on time-dependent, three-dimensional models of mantle convection, *Geophys. Res. Lett., 20*, 2187-2190, 1993.

Turcotte, D.L., and Oxburgh, E.R., Finite amplitude convective cells and continental drift, *J. Fluid Mech., 28*, 29-42, 1967.

Turcotte, D.L., and Schubert, G., Geodynamics: Applications of continuum physics to geological problems, John Wiley and Sons, 1982.

Vangelov, V.I., and Jarvis, G.T., Geometrical effects of curvature in axisymmetric spherical models of mantle convection, *J. Geophys. Res., 99*, 9345-9358, 1994.

Table 1. The viscosity, η, Rayleigh number, $\mathbf{R_a}$, and Nusselt number, Nu, of the models presented in this paper. δ is the thickness of the thermal boundary layer determined from Eq.(2) of the text.

Model	η (Pa s)	$\mathbf{R_a}$ ($\times 10^6$)	Nu	δ (km)
M_1	5×10^{20}	153.39	41.5	21.9
M_2	1×10^{21}	76.70	38.0	27.6
M_3	5×10^{21}	15.30	30.2	47.2
M_4	1×10^{22}	7.67	27.7	59.4
M_5	5×10^{22}	1.53	18.6	101.8
M_6	1×10^{23}	0.767	15.5	127.6
M_7	5×10^{23}	0.153	10.2	219.1
M_8	1×10^{24}	0.0767	7.8	275.9
M_9	5.5×10^{24}	0.0140	4.1	486.4